Electronic Supplementary Material (ESI) for Lab on a Chip.

Electric Supplementary Information

A novel application of hectorite nanoclay for preparation of colorectal cancer spheroids with malignant potential

Yoshihiro Hirade[a], Munehiro Kubota[b], Kaori Kitae[a], Harumi Yamamoto[a], Hiroko Omori[c], Susumu Shinoki[b], Takao Ohmura[d], Kazutake Tsujikawa[e]*

a. Graduate School of Pharmaceutical Science, Osaka University, 1-6 Yamada-oka, Suita City, Osaka 565-0871, Japan.
b. Iwaki Laboratory, Kunimine Industries Co, Ltd, 23-5 Kuidesaku, Shimofunao, Iwaki, Fukushima 972-8312, Japan.
c. Core Instrumentation Facility, Research Institute for Microbial Diseases, Osaka University, 3-1 Yamada-oka, Suita City, Osaka 565-0871, Japan.
d. Kunimine Industries Co, Ltd, 23-5 Kuidesaku, Shimofunao, Iwaki, Fukushima 972-8312, Japan.
e. Graduate School of Pharmaceutical Science, Osaka University, 1-6 Yamada-oka, Suita City, Osaka 565-0871, Japan. E-mail: tujikawa@phs.osaka-u.ac.jp

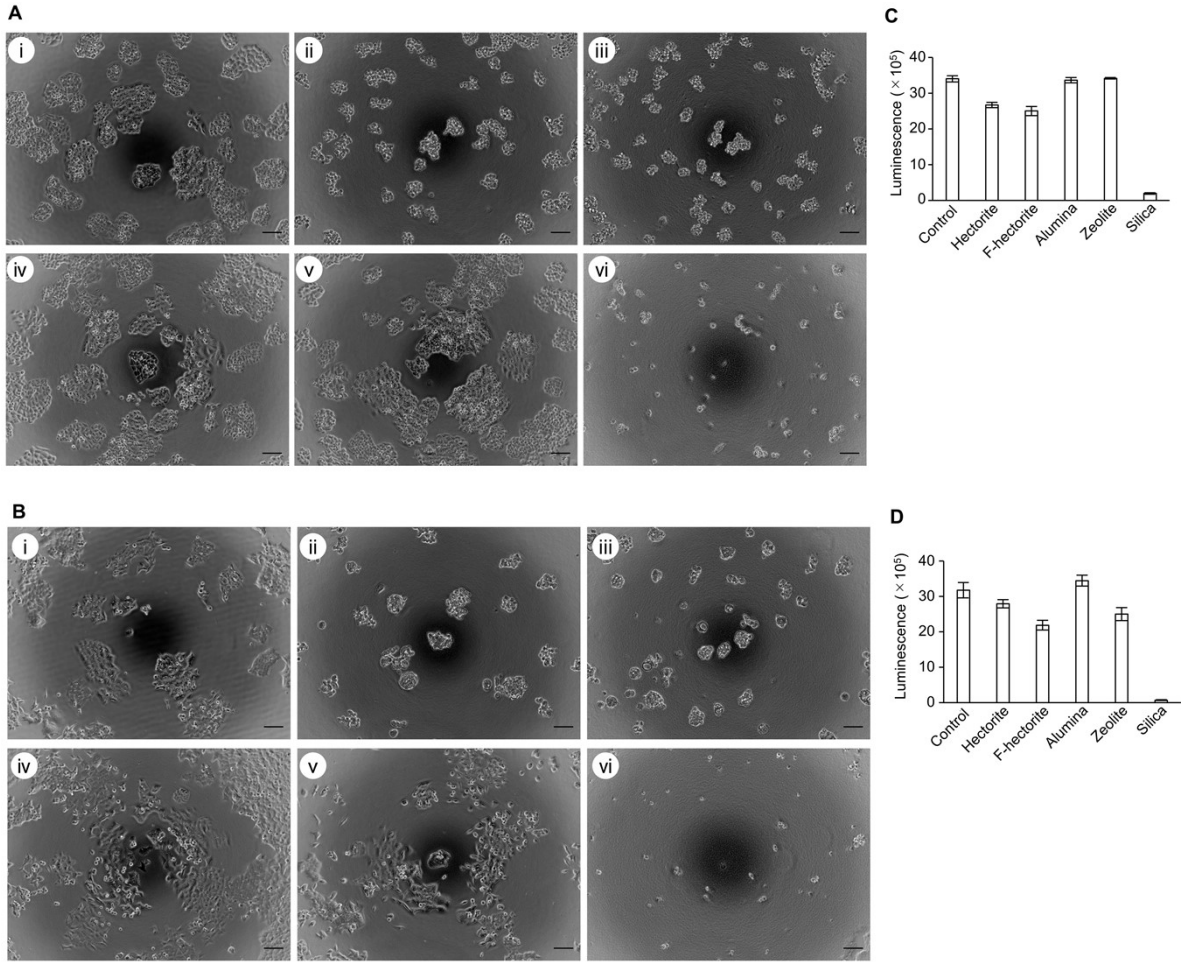

Fig. S1 Morphology of DLD-1 (A) and HCT116 (B) cells cultured in an adherent plate for 4 days in the presence or absence of different minerals at a concentration of 0.01%. Figure notations are the same as in Figure 1. Scale bars indicate 100 μm. Proliferation of DLD-1 (C) and HCT116 (D) cells cultured in an adherent plate for 5 days in the presence or absence of different minerals at a concentration of 0.01%, assessed using an ATP-based luminescence assay. Data are represented as mean ± standard deviation.

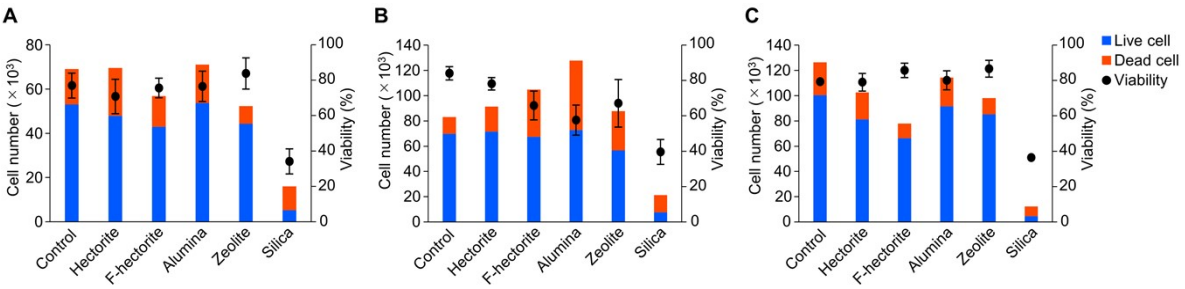

Fig. S2 The number of live and dead cells and the viability of colorectal cancer cells cultured with different minerals. HT-29 (A), DLD-1 (B), and HCT116 (C) were cultured for 5 days in the presence of different minerals at a concentration of 0.01%. The number of live and dead cells and the viability were determined by trypan blue exclusion assay using an automated cell counter. The number of live and dead cells represented as a stacked bar chart is plotted on the primary vertical axis and the viability represented as closed circles is on the secondary vertical axis. Data are expressed as mean ± standard deviation.

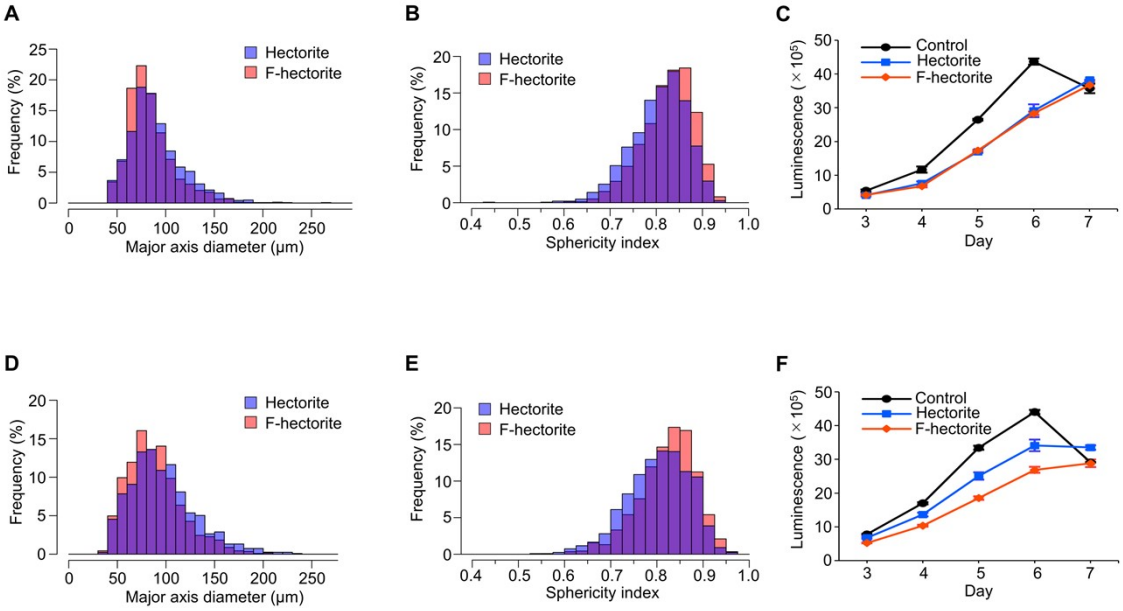

Fig. S3 DLD-1 (A–C) and HCT116 (D–F) cells were cultured in an adherent plate in the presence of 0.01% hectorite or F-hectorite for 4 days. The major axis diameter of each spheroid was measured from micrographs using an image analysis application (A, D). The sphericity index of each spheroid was calculated as described in the Materials and methods section (B, E). Proliferation of DLD-1 (C) and HCT116 (F) cells cultured in an adherent plate in the presence or absence of 0.01% hectorite or F-hectorite, monitored daily using an ATP-based luminescence assay. Data are represented as mean ± standard deviation.

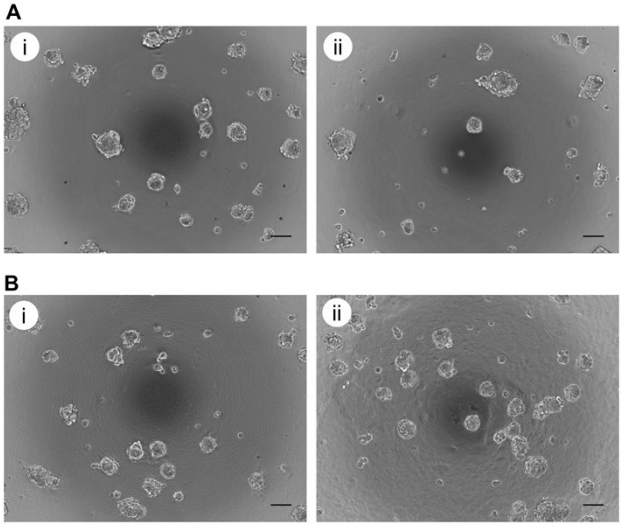

Fig. S4 Images of HT29 spheroids position shift prepared by hectorite and F-hectorite before and after stirring. HT-29 cells were cultured in an adherent plate in the presence of 0.01% hectorite (A) or F-hectorite (B) for 5 days. The microscopy images were captured before (i) and after (ii) stirring by five times pipetting operation. Scale bars indicate 100 μm.

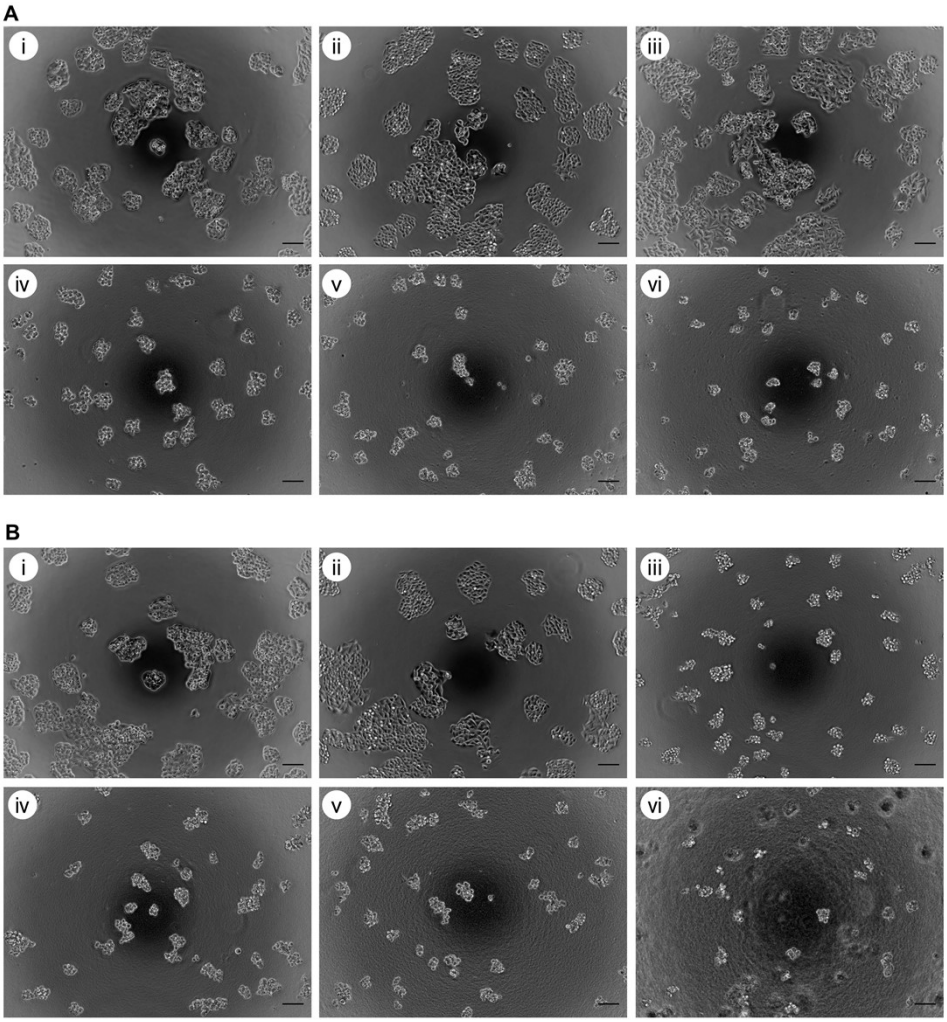
A
i
ii
iii
iv
v
vi
B
i
ii
iii
iv
v
vi
C
Luminescence (× 10⁵)
40
30
20
10
0
Hectorite
F-hectorite
0.00125
0.0025
0.005
0.01
0.02
0.04
Concentration (%)

D

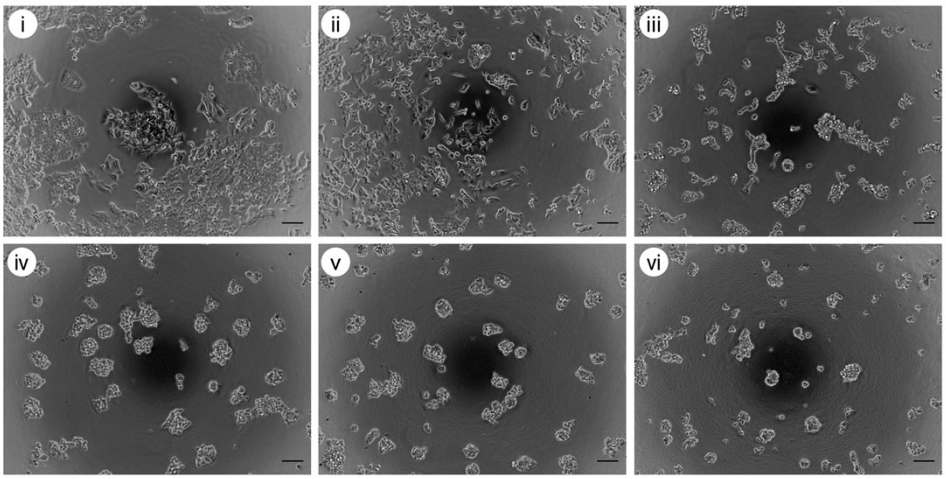
i
ii
iii
iv
v
vi

E

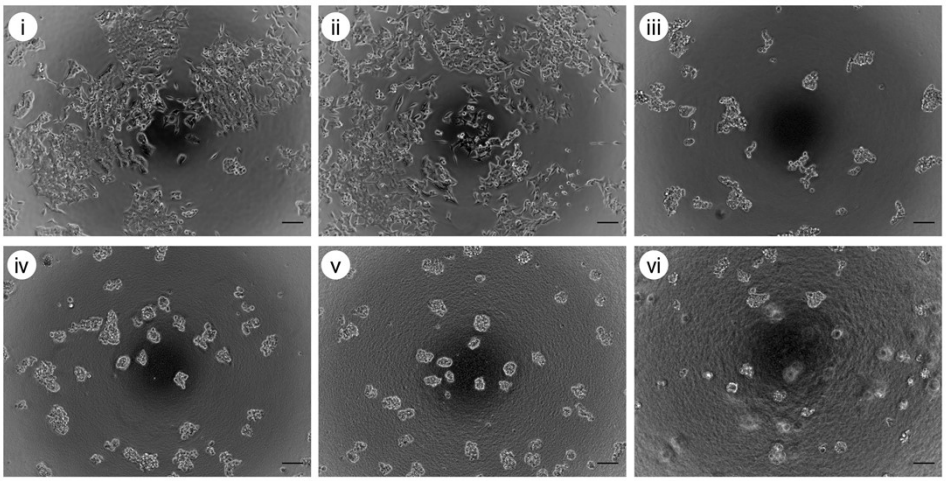
i
ii
iii
iv
v
vi

F

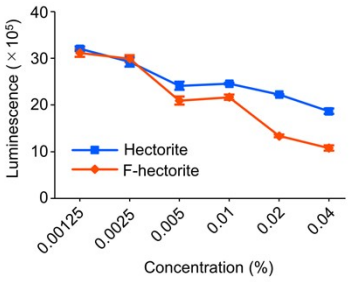
40
30
20
10
0
Luminescence (×10⁵)
Hectorite
F-hectorite
0.00125
0.0025
0.005
0.01
0.02
0.04
Concentration (%)

Fig. S5 Morphology of DLD-1 cells cultured in an adherent plate for 4 days at different concentrations of hectorite (A) or F-hectorite (B); i, 0.00125%; ii, 0.0025%; iii, 0.005%; iv, 0.01%; v, 0.02%; vi, 0.04%. Scale bars indicate 100 μm. (C) Proliferation of DLD-1 cells cultured in an adherent plate for 5 days at different concentrations of hectorite or F-hectorite, assessed using an ATP-based luminescence assay. Data are represented as mean ± standard deviation. Morphology of HCT116 cells cultured in an adherent plate for 4 days at different concentrations of hectorite (D) or F-hectorite (E); i, 0.00125%; ii, 0.0025%; iii, 0.005%; iv, 0.01%; v, 0.02%; vi, 0.04%. Scale bars indicate 100 μm. (F) Proliferation of HCT116 cells cultured in an adherent plate for 5 days under different concentrations of hectorite or F-hectorite, assessed using an ATP-based luminescence assay. Data are represented as mean ± standard deviation.

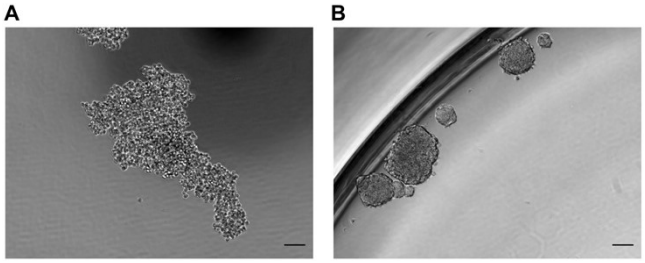

Fig. S6 Morphology of DLD-1 (A) and HCT116 (B) cells cultured in an ultralow adherent plate for 5 days in a medium supplemented with 10% fetal calf serum.

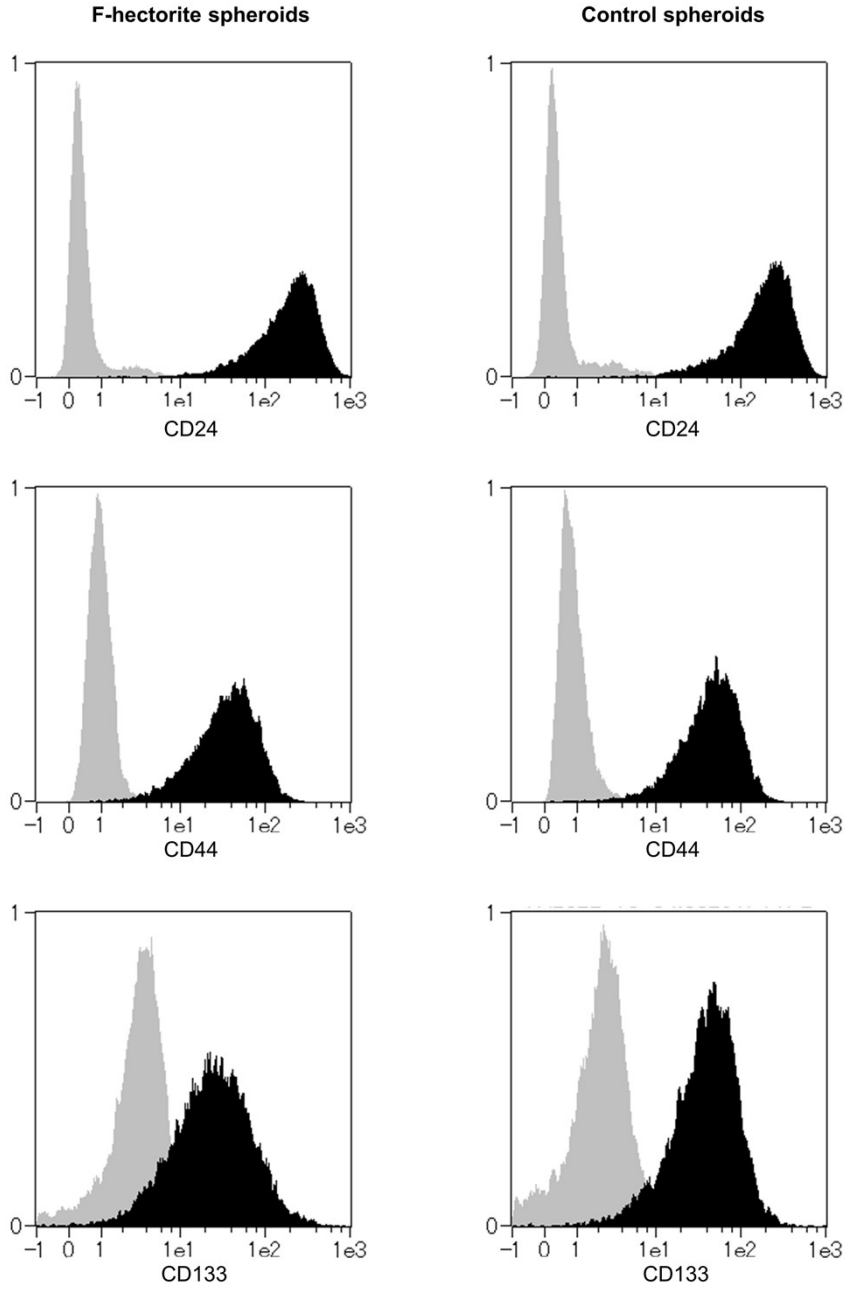

Fig. S7 Expression comparison of CD44, CD24, and CD133 surface markers in HT-29 spheroids prepared by F-hectorite and in an ultralow adherent plate. HT-29 cells were cultured with 0.01% F-hectorite in an adherent plate (F-hectorite spheroids) and in an ultralow adherent plate (Control spheroids), respectively for 5 days. After being dissociated into single cells, the cells were stained with either CD44, CD24 or CD133 antibody and analyzed by flow cytometry. The black and gray shaded histograms represent the analysis with the indicated antibody and a corresponding isotype control antibody, respectively. The number of signal events on the Y-axis was normalized by area.

Table S1 Details of synthetic minerals used in this study

Minerals	Product name	Typical chemical formula	Specific surface area (m^2/g)	BSA adsorption*
Alumina sol	ALUMINASOL-200	Al_2O_3	492.3	452.9
Coloidal silica	SNOWTEX-CXS	SiO_2	475.4	88.9
Hectorite	SUMECTON-SWN	$Na_{0.33}(Mg_{2.67}Li_{0.33})(Si_4O_{10})(OH)_2$	209.4	387.8
Fluoride hectorite	SUMECTON-SWF	$Na_{0.33}(Mg_{2.67}Li_{0.33})(Si_4O_{10})(F,OH)_2$	341.4	484.8
Zeolite	Zeoal 4A	$\{Na_{12}(Al_{12}Si_{12}O_{48})\cdot 27H_2O\}_8$	92.55	14.5

*BSA adsorption amount was expressed as micrograms of BSA per milligrams of inorganic minerals (μg/mg)

Table S2 Summary of quantitative analysis of DLD-1 and HCT116 spheroids formed using 0.01% hectorite minerals

	DLD-1	HCT116
Number of spheroids used for analysis		
Hectorite	1420	1212
F-hectorite	1368	1147
Major axis diameter (μm)		
Hectorite	86 ± 28	73 ± 34
F-hectorite	80 ± 24	69 ± 28
Sphericity index		
Hectorite	0.77 ± 0.060	0.76 ± 0.068
F-hectorite	0.79 ± 0.055	0.78 ± 0.060

Data are shown as median ± standard deviation.

Table S3 Top 30 of the downregulated genes in F-hectorite spheroids compared with that in control spheroids

Gene symbol	Description	Fold change	p-value	FDR p-value
TXNIP	thioredoxin interacting protein	-219.72	1.28E-09	4.56E-06
IFI6	interferon, alpha-inducible protein 6	-61.64	3.43E-10	1.84E-06
LAMP3	lysosomal-associated membrane protein 3	-42.55	4.12E-11	8.84E-07
MX1	MX dynamin-like GTPase 1	-30.8	3.35E-10	1.84E-06
MMP13	matrix metallopeptidase 13	-30.65	3.16E-10	1.84E-06
IFIT1	interferon-induced protein with tetratricopeptide repeats 1	-21.49	4.34E-09	9.31E-06
OAS2	2-5-oligoadenylate synthetase 2	-18.07	2.60E-09	7.97E-06
IFI27	interferon, alpha-inducible protein 27	-16.68	6.76E-10	2.90E-06
NDUFA4L2	NADH dehydrogenase (ubiquinone) 1 alpha subcomplex, 4-like 2	-16.21	4.22E-07	1.00E-04
SERPINE2	serpin peptidase inhibitor, clade E (nexin, plasminogen activator inhibitor type 1), member 2	-14.5	8.67E-09	1.33E-05
EGLN3	egl-9 family hypoxia-inducible factor 3	-14.27	2.01E-08	2.15E-05
CCL20	chemokine (C-C motif) ligand 20	-13.86	9.55E-09	1.37E-05
MT1A	metallothionein 1A	-12.97	4.05E-07	1.00E-04
MX2	MX dynamin-like GTPase 2	-12.15	4.43E-07	1.00E-04
IFI44L	interferon-induced protein 44-like	-11.79	3.65E-09	9.31E-06
MT1L	metallothionein 1L (gene/pseudogene)	-11.3	1.67E-08	2.10E-05
DDX58	DEAD (Asp-Glu-Ala-Asp) box polypeptide 58	-11.18	4.00E-09	9.31E-06
MT1X	metallothionein 1X	-10.78	8.45E-09	1.33E-05
MT2A	metallothionein 2A	-10.65	7.51E-08	5.52E-05
TNFSF10	tumor necrosis factor (ligand) superfamily, member 10	-10.42	1.94E-08	2.15E-05
NDRG1	N-myc downstream regulated 1	-10.36	1.26E-05	1.50E-03
SPINK1	serine peptidase inhibitor, Kazal type 1	-9.83	8.71E-08	6.03E-05
NUCB2	nucleobindin 2	-9.75	1.35E-07	8.01E-05
ARRDC4	arrestin domain containing 4	-9.24	5.08E-09	9.91E-06
OAS1	2-5-oligoadenylate synthetase 1	-9.22	9.42E-08	6.31E-05
CLGN	calmegin	-9.22	6.55E-08	5.02E-05
PARP9	poly(ADP-ribose) polymerase family member 9	-8.98	1.03E-08	1.38E-05
P4HA2	prolyl 4-hydroxylase, alpha polypeptide II	-8.87	2.97E-08	2.75E-05
FXYD3; MIR6887	FXYD domain containing ion transport regulator 3; microRNA 6887	-8.79	6.31E-07	2.00E-04
SP110	SP110 nuclear body protein	-8.36	3.73E-07	1.00E-04

Table S4 Expression of cancer stem cell-related markers in F-hectorite spheroids compared with that in control spheroids

Gene Symbol	Description	Fold change	p-value	FDR p-value
CD24	CD24 molecule	1.64	3.14E-03	5.52E-02
CD44	CD44 molecule (Indian blood group)	2.33	1.17E-03	2.96E-02
CD133	prominin 1	1.32	3.65E-02	2.29E-01

The fold change represents the ratio of F-hectorite to control spheroids.

Table S5 Expression of cadherin and EpCAM molecules in F-hectorite spheroids compared with that in control spheroids

Gene Symbol	Description	Fold change	p-value	FDR p-value
CDH1	cadherin 1, type 1, E-cadherin	1.19	2.30E-01	5.70E-01
CDH2	cadherin 2, type 1, N-cadherin (neuronal)	1.09	7.03E-01	8.92E-01
EPCAM	epithelial cell adhesion molecule	1.11	5.16E-01	7.98E-01

The fold change represents the ratio of F-hectorite to control spheroids.